LIDR 74
CONFID
MARTIN MARIETTA ENERGY SYSTEMS LIBRARIES
3 4456 0360738 1
CENTRAL RESEARCH LIBRARY
DOCUMENT COLLECTION

ORNL 1836
Physics and Mathematics 4a

DECLASSIFIED
CLASSIFICATION CHANGED TO:
BY AUTHORITY OF: TID-1148
BY: 24 Bennette 7/31/57

A MONTE CARLO ESTIMATION OF THE HIGH ENERGY NEUTRON FLUX DISTRIBUTION IN THE ORNL GRAPHITE REACTOR

Jack Moshman

CENTRAL RESEARCH LIBRARY
DOCUMENT COLLECTION
LIBRARY LOAN COPY
DO NOT TRANSFER TO ANOTHER PERSON
If you wish someone else to see this document, send in name with document and the library will arrange a loan.

OAK RIDGE NATIONAL LABORATORY
OPERATED BY
CARBIDE AND CARBON CHEMICALS COMPANY
A DIVISION OF UNION CARBIDE AND CARBON CORPORATION
UCC
POST OFFICE BOX P
OAK RIDGE, TENNESSEE

RESTRICTED DATA
This document contains Restricted Data as defined in the Atomic Energy Act of 1954. Its transmittal or the disclosure of its contents in any manner to an unauthorized person is prohibited.
CONFIDENTIAL

ORNL 1836

[redacted]

[redacted] This document consists of 32 pages.
Copy 4 of 181 copies. Series A.

Contract No. W-7405-eng-26

A MONTE CARLO ESTIMATION OF THE HIGH ENERGY NEUTRON FLUX DISTRIBUTION IN THE ORNL GRAPHITE REACTOR

by

Jack Moshman

DATE ISSUED

FEB 8 1955

[redacted]

Oak Ridge National Laboratory
operated by
CARBIDE AND CARBON CHEMICALS COMPANY
A Division of Union Carbide and Carbon Corporation
Post Office Box P
Oak Ridge, Tennessee

[redacted]

MARTIN MARIETTA ENERGY SYSTEMS LIBRARIES
3 4456 0360738 1

INTERNAL DISTRIBUTION

1. C. E. Center
2. Biology Library
3. Health Physics and Metallurgy Library
4-5. Central Research Library
6. Reactor Experimental Engineering Library
7-13. Laboratory Records Department
14. Laboratory Records, ORNL R.C.
15. C. E. Larson
16. L. B. Emlet (K-25)
17. J. P. Murray (Y-12)
18. A. M. Weinberg
19. E. H. Taylor
20. E. D. Shipley
21. A. S. Householder
22. F. C. VonderLage
23. C. P. Keim
24. W. H. Jordan
25. J. A. Swartout
26. S. C. Lind
27. F. L. Culler
28. R. S. Livingston
29. A. H. Snell
30. A. Hollaender
31. M. T. Kelley
32. G. H. Clewett
33. J. H. Frye, Jr.
34. K. Z. Morgan
35. T. A. Lincoln
36. C. S. Harrill
37. D. W. Cardwell
38. C. E. Winters
39. E. M. King
40. Lewis Nelson
41. D. D. Cowen
42. J. A. Lane
43. R. A. Charpie
44. S. J. Cromer
45. M. J. Skinner
46. G. C. Williams
47. S. G. Campbell
48. C. L. Bradshaw
49. N. M. Dismuke
50. M. R. Arnette
51. S. E. Atta
52. J. Z. Hearon
53. ORNL Document Reference Library, Y-12 Branch

EXTERNAL DISTRIBUTION

54. AF Plant Representative, Burbank
55. AF Plant Representative, Seattle
56. AF Plant Representative, Wood-Ridge
57. American Machine and Foundry Company
58. ANP Project Office, Fort Worth
59-63. Argonne National Laboratory
64. Armed Forces Special Weapons Project (Sandia)
65. Army Chemical Center
66-68. Atomic Energy Commission, Washington
69. Babcock and Wilcox Company
70. Battelle Memorial Institute
71. Bendix Aviation Corporation
72-75. Bettis Plant (WAPD)
76-78. Brookhaven National Laboratory
79. Bureau of Ships
80. Carbide and Carbon Chemicals Company (C-31 Plant)
81-82. Carbide and Carbon Chemicals Company (K-25 Plant)
83. Chicago Patent Group
84. Chief of Naval Research
85. Columbia University (Havens)
86-87. Commonwealth Edison Company
88. Department of the Navy - Op-362
89. Detroit Edison Company

[redacted]

90. Directorate of Research (WADC)
91-93. duPont Company, Augusta
94. Duquesne Light Company
95. Engineer Research and Development Laboratories
96. Foster Wheeler Corporation
97-100. General Electric Company (ANPD)
101. General Electric Company (APS)
102-109. General Electric Company, Richland
110-111. Goodyear Atomic Corporation
112. Hanford Operations Office
113. Headquarters, Air Force Special Weapons Center
114. Iowa State College
115. Kaiser Engineers
116-119. Knolls Atomic Power Laboratory
120-121. Los Alamos Scientific Laboratory
122. Monsanto Chemical Company
123-124. Mound Laboratory
125. National Advisory Committee for Aeronautics, Cleveland
126. National Bureau of Standards
127. Naval Medical Research Institute
128-129. Naval Research Laboratory
130. New Brunswick Laboratory
131. Newport News Shipbuilding and Dry Dock Company
132. New York Operations Office
133-135. North American Aviation, Inc.
136. Nuclear Development Associates, Inc.
137. Nuclear Metals, Inc.
138. Pacific Northwest Power Group
139. Patent Branch, Washington
140. Pennsylvania Power and Light Company
141. Powerplant Laboratory (WADC)
142-145. Phillips Petroleum Company (NRTS)
146. Pratt & Whitney Aircraft Division (Fox Project)
147. Sandia Corporation
148. Tennessee Valley Authority (Dean)
149. USAF Project Rand
150. U. S. Naval Postgraduate School
151. U. S. Naval Radiological Defense Laboratory
152. UCLA Medical Research Laboratory
153-155. University of California Radiation Laboratory, Berkeley
156-159. University of California Radiation Laboratory, Livermore (1 copy to E. J. Leshan)
160-161. University of Rochester
162. Vitro Engineering Division
163. Walter Kidde Nuclear Laboratories, Inc.
164. Westinghouse Electric Corporation (IAPG)
165. Yale University
166-180. Technical Information Service, Oak Ridge
181. Division of Research and Medicine, AEC, ORO

[redacted]

[redacted]

A MONTE CARLO ESTIMATION OF THE HIGH ENERGY NEUTRON FLUX DISTRIBUTION IN THE ORNL GRAPHITE REACTOR

Statement of the Problem

It was desired to estimate the proportion of the fast neutron flux as a function of energy in various regions of the ORNL graphite reactor lattice. The regions chosen as representative of those of interest are numbered I, II and III in the schematic diagram (Figure 1) of a cross-sectional view of the pile.

Fast neutrons were taken to be those with an energy in excess of .025 Mev. Neutrons with energies in excess of .025 Mev were classified into 14 energy intervals. The classification referred to a specific neutron flight between collisions so that, in general, from the birth of a neutron to its degradation to an energy of less than .025 Mev it passed through various intervals. The selected energy intervals, not inclusive of the upper limit, were:

1)	.025	-	.05	Mev
2)	.05	-	.1	Mev
3)	.1	-	.25	Mev
4)	.25	-	.5	Mev
5)	.5	-	1.0	Mev
6)	1.0	-	2.0	Mev
7)	2.0	-	3.0	Mev
8)	3.0	-	4.0	Mev
9)	4.0	-	5.0	Mev
10)	5.0	-	6.0	Mev
11)	6.0	-	7.0	Mev
12)	7.0	-	8.0	Mev
13)	8.0	-	9.0	Mev
14)	9.0	-	10.0	Mev

UNCLASSIFIED
ORNL-LR-DWG 2344

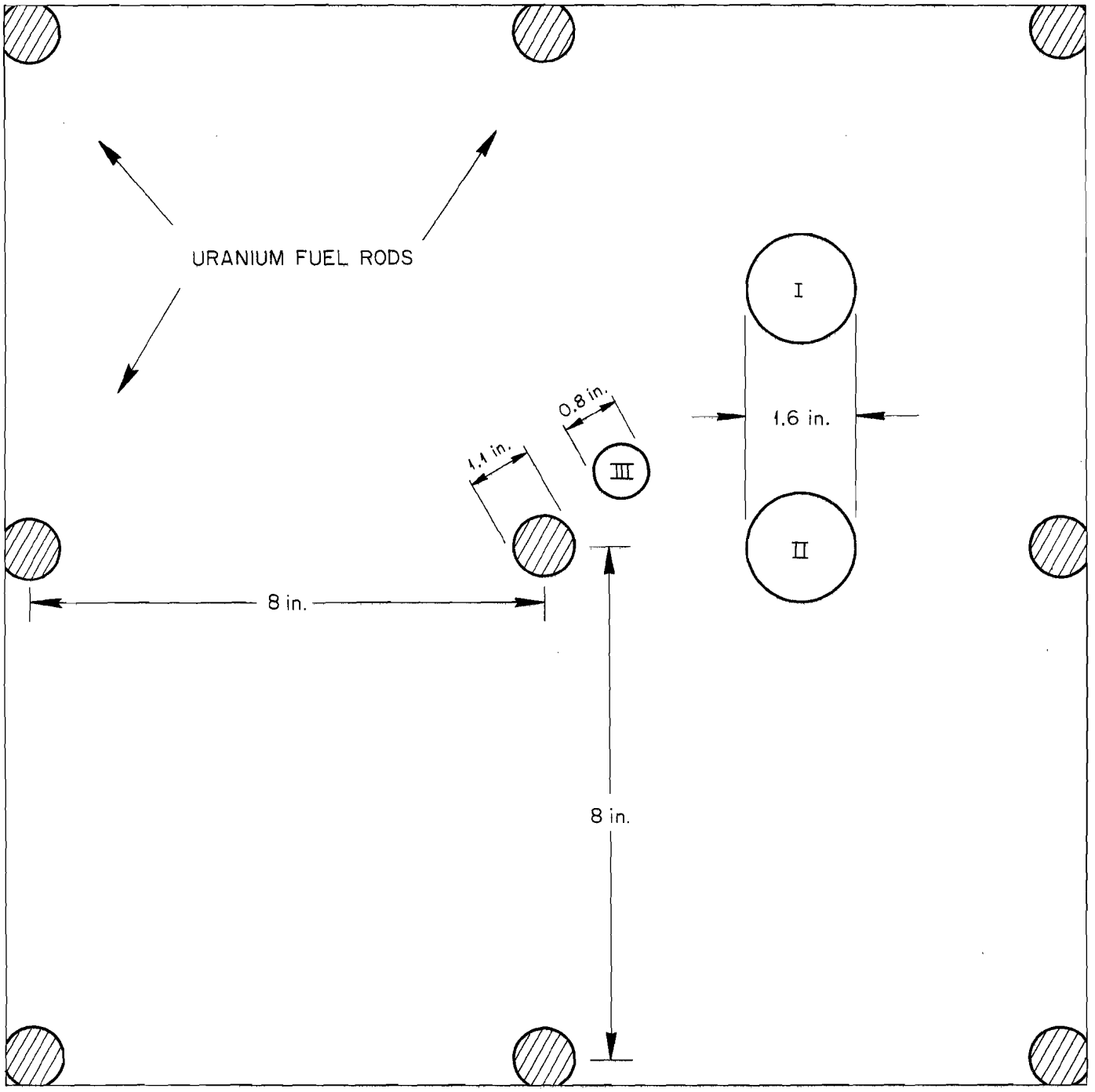

Fig. 1. Schematic Cross-Sectional View of ORNL Pile.

[redacted]

The original energy spectrum was truncated at 10 Mev.

Sources of Data

1. Energy Spectrum. The distribution of energies possessed by the neutrons being born in the uranium rods was taken to be that given by

$$\varphi(E) = \sqrt{\frac{\pi e}{2}}\; e^{-E} \sinh \sqrt{2E} \tag{1}$$

so that the probability of a neutron being born with energy less than E_o is

$$\text{Prob}\left\{E \leqslant E_o\right\} = \Phi(E_o) = \int_0^{E_o} \varphi(E)\, dE\,. \tag{2}$$

The probability distribution, $\varphi(E)$, is depicted in Figure 2.

2. Neutron Origin. Each neutron is taken to originate in a rod with polar coordinates (r, θ). If a cross-sectional view of a fuel rod is considered as in Figure 3, it was assumed that the angle θ is uniformly distributed over the interval $(0, 2\pi)$ and the radius vector r is proportional to

$$I_o(\mathcal{H}\, r) \approx 1 + \frac{(\mathcal{H}\, r)^2}{4} + \frac{(\mathcal{H}\, r)^4}{64} \tag{3}$$

where $\mathcal{H} = .6306$ and r is in centimeters.

3. Uranium Cross Sections. Total uranium cross sections $\sigma_t(U)$ were partitioned into elastic scattering cross sections $\sigma_e(U)$, inelastic scattering cross sections $\sigma_i(U)$ and absorption cross sections $\sigma_a(U)$ which included fission as well as non-productive capture. Thus

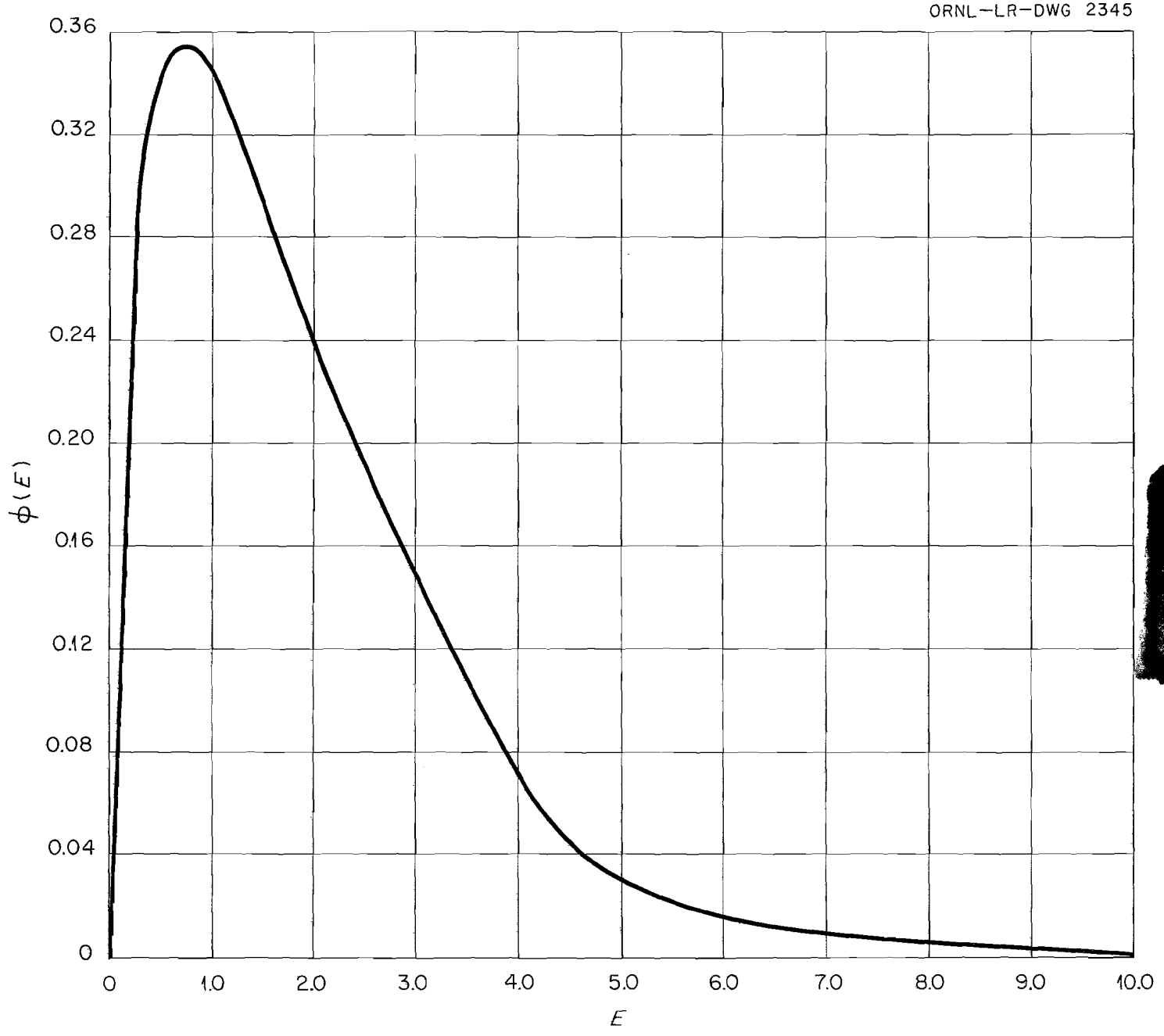

Fig. 2. Probability Distribution, $\phi(E)$, of Initial Energies.

UNCLASSIFIED
ORNL-LR-DWG 2346

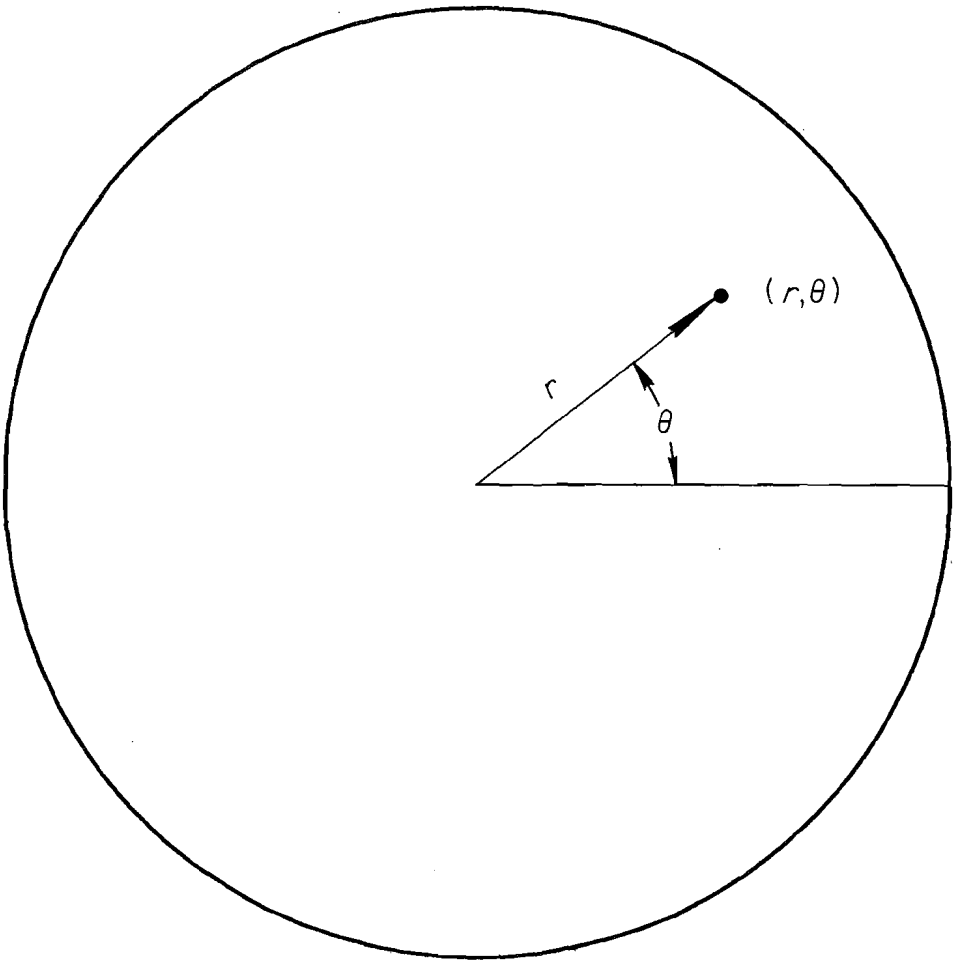

Fig. 3. Cross Section of Fuel Rod With Coordinates of Point of Origin.

$$\sigma_t(U, E) = \sigma_e(U, E) + \sigma_i(U, E) + \sigma_a(U, E) \tag{4}$$

where the functional dependence on energy is indicated in (4). Various sources were used to estimate the total cross sections, in particular ORNL-86 [1]. Analytic approximations to σ_e and σ_i were taken to be

$$\sigma_e(U, E) = \begin{cases} 4 + \dfrac{.62}{E} & .10 \leqslant E < 10.00 \\ 14.5 - 43\,E & .025 < E \leqslant .10 \end{cases} \tag{5}$$

and

$$\sigma_i(U, E) = \begin{cases} 2 - \dfrac{.8}{E} & .4 \leqslant E < 10.0 \\ 0 & .025 < E \leqslant .4 \end{cases} \tag{6}$$

respectively, and σ_a was taken to be .7 for all E. All cross sections are in barns. Partial inelastic cross sections for scattering into a given energy ranges were provided by Holmes [2] from some data given by Weisskopf and Bethe. The data used are tabulated in Table I. The quantity p is the percentage of $\sigma_i(U, E)$ for scattering into the given energy range.

Table I

Percentage of Inelastic Cross Sections for Scattering into Specified Energy Ranges.

Incident Energy (Mev)	Percentage of σ_i (U, E) (p)	Resulting Energy Range (Mev)
.5	100	.25
1.0	50	0 - .50
	50	.50 - .75
2.0	50	0 - .50
	30	.50 -1.00
	15	1.00-1.50
	5	1.50-2.00
3.0	60	0 - .75
	20	.75 -1.50
	15	1.50-2.25
	5	2.25-3.00
5.0	40	0 - .50
	30	.50 -1.00
	20	1.00-2.00
	10	2.00-3.00
	0	3.00-5.00

4. Carbon Cross Sections. Primary data for the cross sections of the graphite came from the Project Handbook [3]. In view of the various resonance regions, the energy scale was divided into seven sections and a polynomial of second or lower degree was fitted in each section. It has been assumed that $\sigma_t = \sigma_e = \sigma$ for carbon. The analytic expressions are:

$$\sigma(C, E) = \begin{cases} 1.700\,E^2 - 3.950\,E + 4.700 & .025 \leqslant E < 1 \\ .292\,E^2 - 1.675\,E + 3.833 & 1 \leqslant E < 2 \\ -.050\,E + 1.750 & 2 \leqslant E < 3 \\ -3.458\,E^2 + 24.656\,E - 41.396 & 3 \leqslant E < 4 \\ -2.595\,E^2 + 22.707\,E - 47.408 & 4 \leqslant E < 5 \\ -.200\,E + 2.200 & 5 \leqslant E < 6 \\ 1.000 & 6 \leqslant E < 10 \end{cases} \quad (7)$$

The cross section curve for carbon is plotted in Figure 4.

General Procedure

The flux through a given region is proportional to the total lengths of the neutron flight paths that intersect that region. The analytical Monte Carlo procedure manufactured neutron flight paths and totaled the lengths of all paths intercepted by the regions illustrated in Figure 1. The procedure was designed to utilize the various symmetries in the lattice.

Consider a portion of the lattice whose planar cross-section is shown in Figure 5. If R is the region in which the flux is to be estimated and F the fuel rod in which the neutron originated, then flight path P results in an intercepted length whose reflection in the plane is ℓ . On the other hand flight path P' intercepts R' with length ℓ' . R' is not the region to be studied, but a translation of flight path P' to F' would result in the neutron

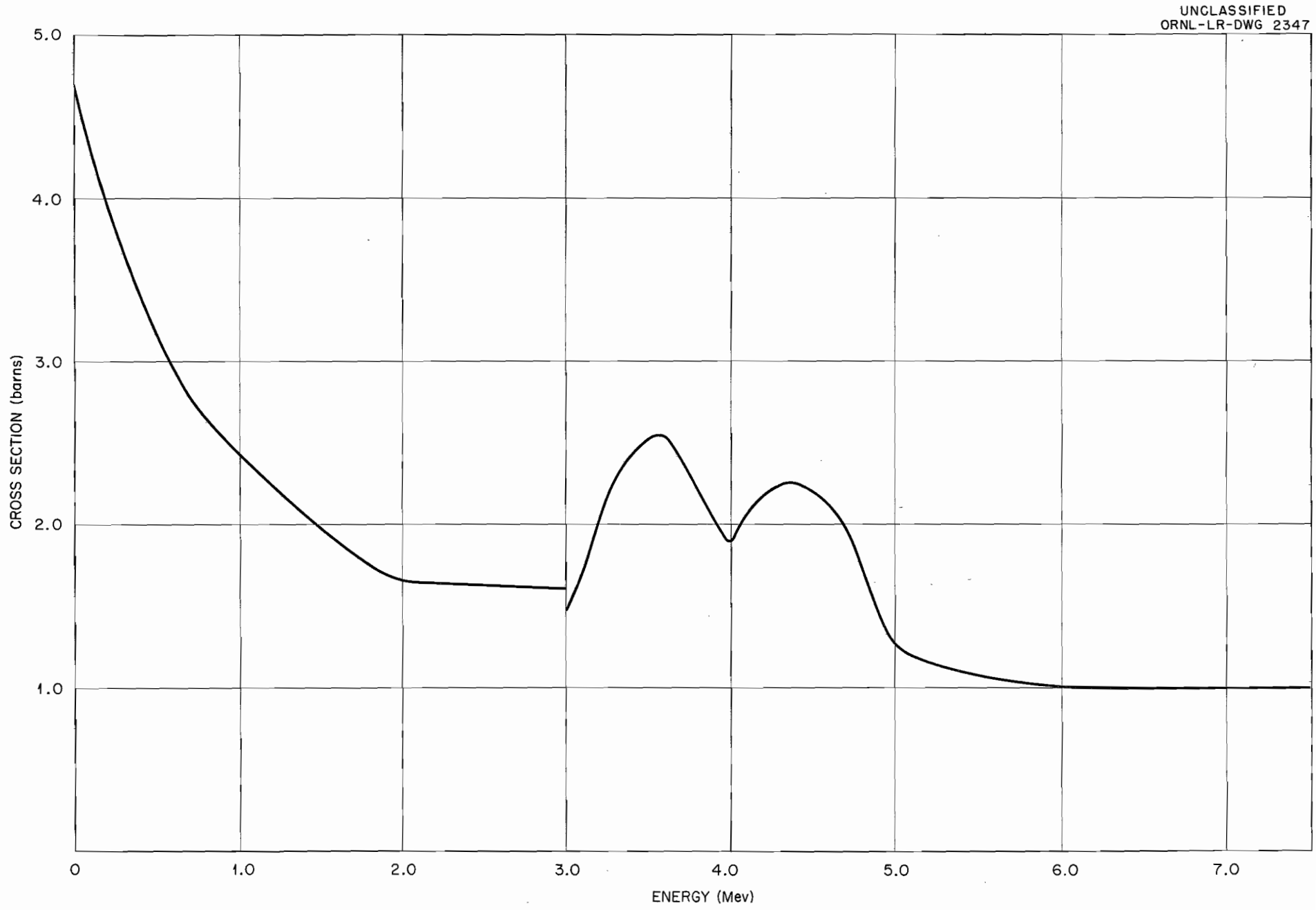

Fig. 4. Carbon Cross Section Curve Derived from Equation 7.

UNCLASSIFIED
ORNL-LR-DWG 2348

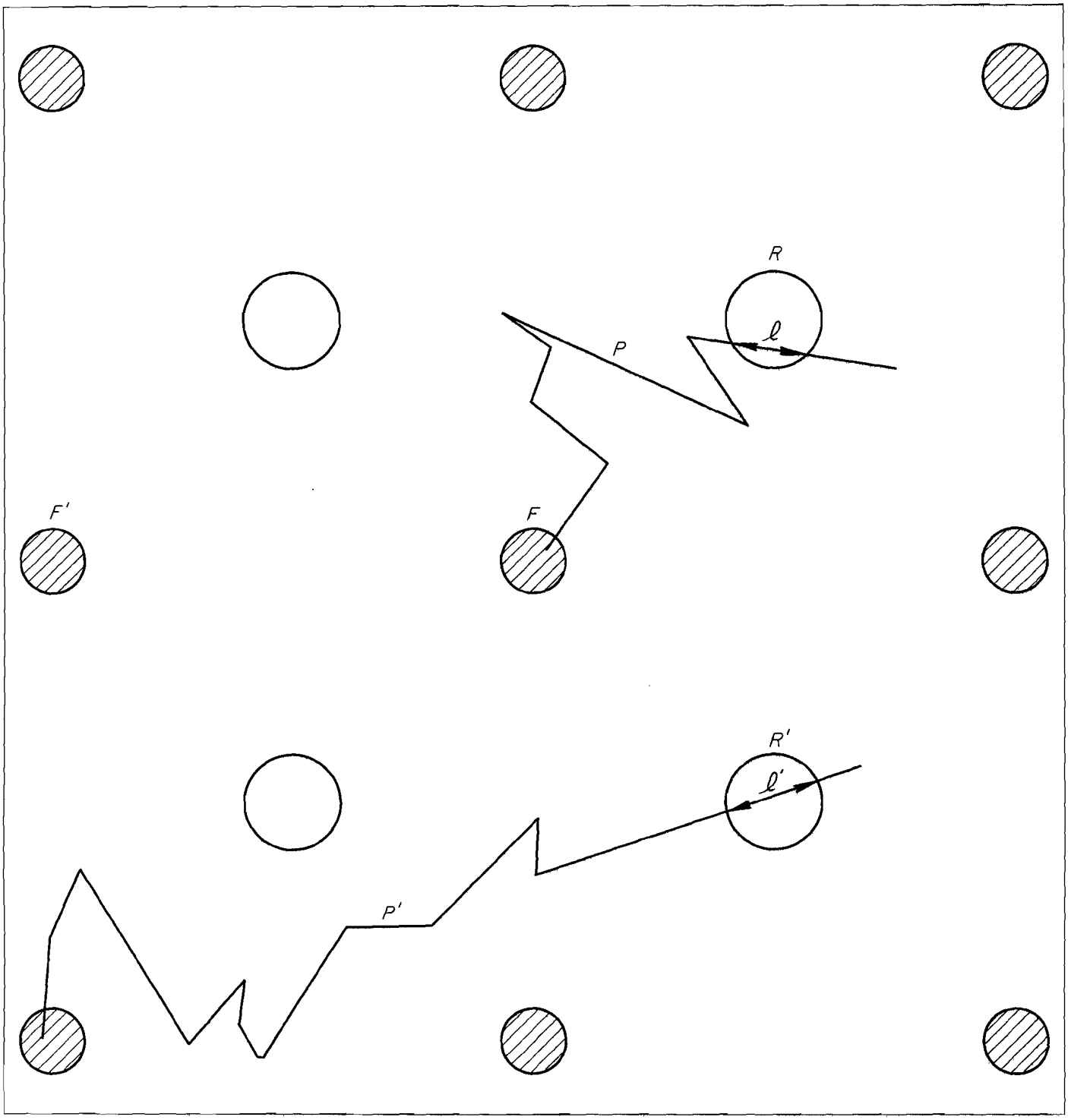

Fig. 5. Schematic Diagram Indicating Translation of Flight Path Because of Lattice Symmetry.

intercepting R . The origin in F was arbitrary. For each neutron originating in F another could, with equal probability, have originated in F' with parallel paths. Hence counting ℓ' in R' towards the total flux is equivalent to starting a neutron at F' . Thus consideration of all regions symmetric to R with respect to the fuel rod lattice is equivalent to originating neutrons at all rods and considering only their interceptions in R .

In a similar manner one may take advantage of the symmetry along the fuel rod. Instead of permitting neutrons to be born uniformly along an uranium rod and to calculate the lengths of the flight paths intercepted in specific small region, it was more convenient to adopt the following procedure.

All neutrons are considered to originate in a plane disc at the center of a rod. Lengths of its flight path intercepted by a cylinder, parallel to the fuel rod, with radius equal to that of the region under investigation and whose length is the same as that of a fuel rod, are calculated. The same length is obtainable from parallel paths originating elsewhere in the fuel rod and passing through the specified region.

In summary, the general procedure adopted was to consider all neutrons as originating in a plane disc in one fuel rod. By considering the length intercepted in all regions symmetric to the one in question, flux estimates were obtained assuming neutrons originated in any rod, not too near the side of the pile, and at any distance from the disc.

The Machine Procedure

The problem was first considered for attack on the IBM Card Programmed

Calculator (CPC). The procedure was coded and run. It was found that the time necessary to follow a neutron through a complete history was in the order of 20 minutes. A run of 25 histories in an 8 hour shift was optimal, but rarely attained because of mechanical and scheduling difficulties. A total of 100 basic histories was completed and the decision was made to recode the problem for the UNIVAC. Preliminary CPC results indicated that about 7500 histories would be necessary to attain 5 per cent accuracy in the final result.

The problem was coded in two parts. The first part consisted of the generation of 10,000 histories. Each collision was noted and stored on a total of ten magnetic tapes with the following information:

a) History number

b) Collision number

c) Energy after collision

d) Space coordinates.

A rectangular coordinate system was used. The (x, y) plane was the plane of the disc in which all neutrons originated. The z axis was coincident with the axis of the cylindrical fuel rod. It was found that the UNIVAC averaged about 200 histories per hour and about 50 hours of machine time was consumed in obtaining the 10,000 histories.

The second part consisted of determining whether or not the path between two consecutive collisions of the same neutron passed through the region of interest or one symmetric to it. The second part was in fact done three times, once for each of the regions depicted in Figure 1.

The second part consumed about 4 hours per region, but was beset by some unexpected magnetic tape difficulties on the UNIVAC. In some cases the tapes

were torn and had to be spliced and in other instances whole tapes could not be read into the machine because of discrepancies in the pulse checking system of the UNIVAC. Of the 10,000 histories, about 9600 were used for region I, 7700 for region II and 7650 for region III. The numbers are, of necessity, approximate, but correct to within negligible error since the final results are expressible in ratios rather than absolute averages.

Generation and Application of Random Numbers

In any Monte Carlo procedure copious amounts of random numbers are consumed. This problem was no exception; some 3×10^6 numbers were required. In order to obtain a sequence of numbers that would not be cyclic of order less than 3×10^6, the generating procedure described by Moshman [4] was used. This guaranteed 5×10^8 numbers before the repetition of a cycle.

The random numbers generated in the above manner may be multiplied by a constant and used directly in sampling from a uniform distribution. In some cases one can analytically transform a random number R into a random variate from another distribution. For example if

$$d\,F(x) = a\,e^{-ax}\,dx \qquad 0 \leqslant x < \infty \tag{8}$$

then one may find the value of x, say x_1, corresponding to a random number R_1 by letting

$$R_1 = \int_0^{x_1} a\,e^{-ax}\,dx \tag{9}$$

obtaining

$$x_1 = -\frac{1}{a} \ln (1 - R_1) \tag{10}$$

or equivalently

$$x_1 = -\frac{1}{a} \ln R \quad . \tag{11}$$

In a distribution such as that given in (1), a different procedure was followed. Draw two random numbers, R_1 and R_2 and see if

$$p\, \varphi(q\, R_1) \geqslant R_2 \tag{12}$$

where $\frac{1}{p}$ is the maximum ordinate of $\varphi(E)$ and q is some convenient point of truncation of the range of E. In this case $q = 10$ Mev. If (12) is satisfied then $q\, R_1$ is taken to be a random number drawn from $\varphi(E)$. If

$$p\, \varphi(q\, R_1) < R_2 \tag{13}$$

then R_1 and R_2 are discarded and a new pair R_1' and R_2' selected and the procedure repeated. It may be shown that the derived sequence of acceptable numbers does have the distribution $\varphi(E)$.

Generating a Sample History

The generation of a sample flight is best followed by means of a general flow chart such as is shown in Figure 6. An initial energy, E_o, is selected as in the manner shown in the previous section. The radial distance r from the center of the originating fuel rod is chosen proportional to (3). A random number, R_1, is chosen and the coordinates of the place of birth of the neutron are taken to be

$$\begin{aligned} x &= r \cos \frac{\pi}{2} R_1 \\ y &= r \sin \frac{\pi}{2} R_1 \\ z &= 0 \quad . \end{aligned} \tag{14}$$

Randomly chosen direction cosines determine the direction of flight. Denote the direction cosines by ℓ_o, m_o and n_o. These are selected by drawing 3 random numbers R_2, R_3 and R_4. If

$$R_2^2 + R_3^2 + R_4^2 = S^2 \leqslant 1 \tag{15}$$

then

$$\left.\begin{aligned} \ell_o &= \frac{R_2}{S} \\ m_o &= \frac{R_3}{S} \\ n_o &= \frac{R_4}{S} \end{aligned}\right\} \quad . \tag{16}$$

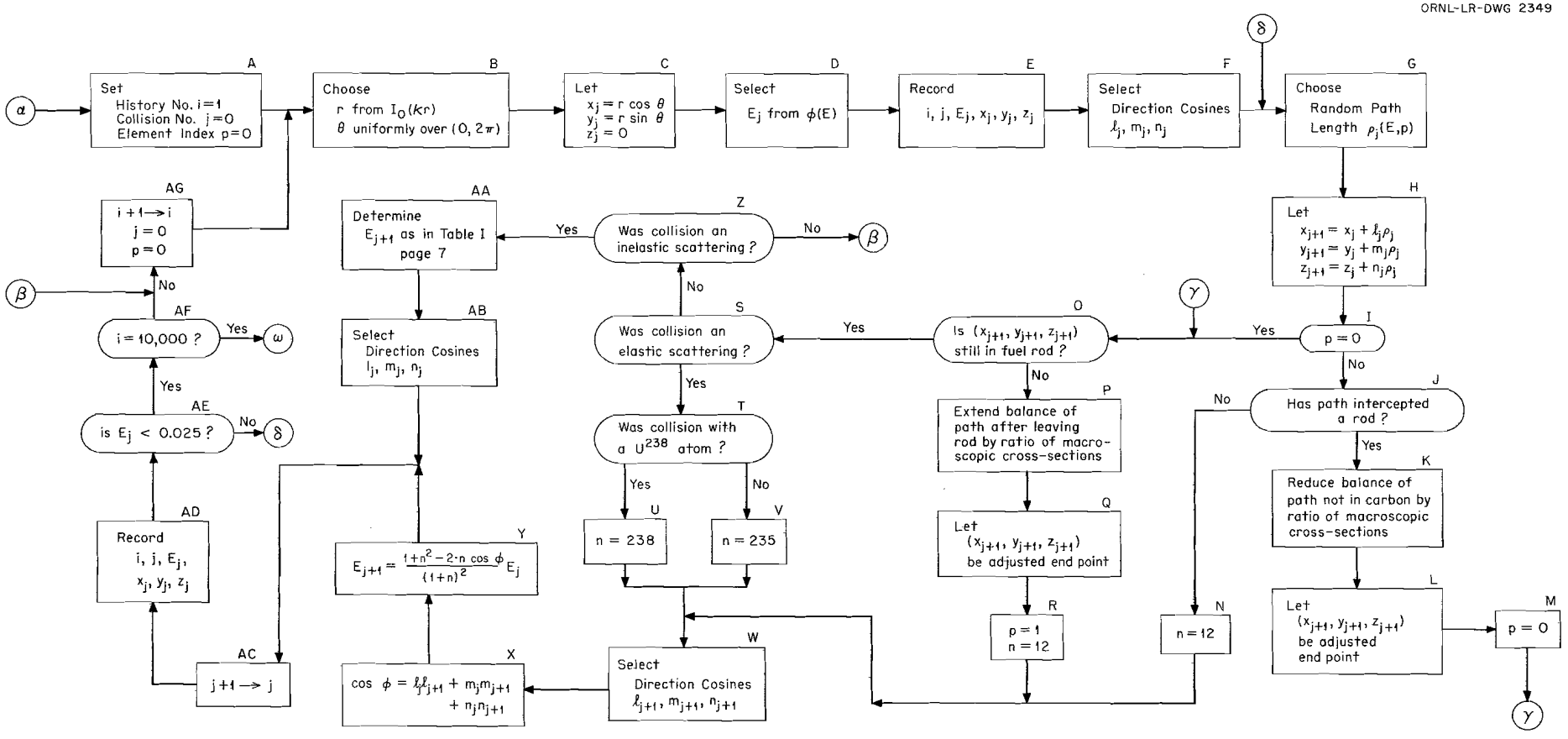

Fig. 6. Schematic Flow Chart of Main Routine.

If $S^2 > 1$, then another triplet is drawn and inequality (15) re-examined. The inequality test is necessary for otherwise all directions would not be equiprobable. This is easily seen if one considers the random triplet to determine a point in the unit sphere and the direction to coincide with a vector drawn to the point from the center of the sphere. If the point were permitted to be anywhere in a unit cube, then there would be a preferential orientation in the direction of the vertices.

Having an energy and direction, a path length is sampled from the appropriate exponential distributions and the coordinates of the apparent collision determined. If the point of apparent collision is still within the rod, one selects a new set of direction cosines ℓ_1, m_1, n_1 and then examines the type of collision. This is accomplished by selecting another random number R_5 and seeing if

$$\frac{\sigma_e(U, E_o)}{\sigma_t(U, E_o)} \geqslant R_5 \tag{17}$$

or

$$\frac{\sigma_e(U, E_o) + \sigma_i(U, E_o)}{\sigma_t(U, E_o)} \geqslant R_5 > \frac{\sigma_e(U, E)}{\sigma_t(U, E)} \tag{18}$$

or

$$1 \geqslant R_5 > \frac{\sigma_e(U, E_o) + \sigma_i(U, E_o)}{\sigma_t(U, E_o)} \tag{19}$$

If (17) holds, an elastic scattering is assumed to have taken place and, defining

$$\cos \varphi = \ell_o \ell_1 + m_o m_1 + n_o n_1 \quad , \tag{20}$$

the new energy E_1 is

$$E_1 = \frac{238^2 + 1^2 - (2)(238) \cos \varphi}{(238 + 1)^2} E_o \tag{21}$$

or

$$E_1 = \frac{235^2 + 1^2 - 2(235) \cos \varphi}{(235 + 1)^2} E_o \tag{22}$$

depending upon whether the collision was with a U^{238} or a U^{235} atom. This latter choice again calls for a random number and determining if it is less than .993, the relative abundance of U^{238}, or not respectively.

If (18) obtains, the new energy is taken to be distributed according to Table I. Two random numbers, R_6 and R_7, are selected; the first determines the energy range of the departing neutron in an obvious way, the second determines the new energy uniformly in the selected range. For example, if $E_o = 2$ Mev, $R_6 = .6174$ and $R_7 = .3892$ then the second energy range is chosen $(.50 < R_6 \leqslant .50 + .30)$ and $E_1 = .50 + .50 R_7$.

If (19) holds, a new history is started.

In the event that the point of apparent collision was outside the fuel rod, the distance from the point of exit to the point of apparent collision is extended by a factor equal to the ratio of the uranium to the carbon macroscopic cross sections.

A collision in the graphite is always assumed to be an elastic scattering so that after choice of the new direction cosines, the new energy is

$$E_1 = \frac{12^2 + 1^2 - 24 \cos \varphi}{(12 + 1)^2} E_o \tag{23}$$

and the process repeated.

At each apparent collision two possibilities that require special treatment may occur: 1) The path may pass the interface between the uranium and the carbon; or 2) The new energy may be less than .025 Mev.

In the event of the first case, the neutron path is extended or shortened by the appropriate ratio of macroscopic cross sections. It is necessary also to consider the possibility that a neutron may pass clear through a rod.

If the energy is degraded below .025 Mev the history is terminated and a new one started.

Estimation of the Flux

The coordinate system was chosen with a unit equal to 8 inches, the lattice dimension. In obtaining the lengths of the neutron paths intercepted by cylinders placed at the three points described in an earlier section, a determination was first made as to whether or not a flight path intercepted a cylinder

between successive collisions. This was easily done by considering the projection of the line of flight in the (x, y) plane and translating the coordinates to place the origin at the center of one of the circles projected by the cylinders. If (x_1, y_1) and (x_2, y_2) are two consecutive collision points determining the line in the (x, y) plane the equation of the line is

$$\frac{x - x_1}{x_2 - x_1} = \frac{y - y_1}{y_2 - y_1} \tag{24}$$

or

$$\frac{x}{x_2 - x_1} - \frac{y}{y_2 - y_1} + \frac{y_1(x_2 - x_1) - x_1(y_2 - y_1)}{(x_2 - x_1)(y_2 - y_1)} = 0 \tag{25}$$

which may be considered as the normal form of the straight line

$$\triangle y\, x - \triangle x\, y - p = 0 \tag{26}$$

say. Let $D = \sqrt{(\triangle x)^2 + (\triangle y)^2}$. Then the distance d from any point (x^o, y^o) to the line is

$$d = -\frac{\triangle y}{D} x^o + \frac{\triangle x}{D} y^o + \frac{p}{D} \quad . \tag{27}$$

The pair (x^o, y^o) is permitted to run over the integers between (x_1, y_1) and (x_2, y_2) and to cover also those integers which are included within a distance

no greater than the radius, r_o, of the regions in Figure 1 from (x_1, y_1) and (x_2, y_2). If any d so obtained is less than r_o, then the flight path must have intersected the cylindrical region.

A decision is then made as to whether none, one or both end points are in the region and the appropriate length is calculated. The general nature of these calculations are illustrated in the flow chart in Figure 7.

Statistical Analysis of the Data

Let F_{ij} be the sum of lengths intercepted in region i (or one symmetric to it) of neutrons in the energy range ΔE_j. Then F_{ij} is proportional to the flux of neutrons through region i having energies in ΔE_j. Let $F_i = \sum_j F_{ij}$ so that F_i is proportional to the total fast flux in region i. Then, if N is the total number of neutron histories,

$$R_{ij} = \frac{F_{ij}/N}{F_i/N} = \frac{F_{ij}}{F_i} \tag{28}$$

is the proportion of the total flux in region i. The distribution of R_{ij} as a function of energy is desired for the three $(i = I, II, III)$ regions. If F_{ijk} is the contribution to F_{ij} from the kth $(k = 1, 2, \ldots, N)$ neutron, an estimate of the variance of F_{ij}/N is

$$s^2_{F_{ij}/N} = \frac{N \sum_k F^2_{ijk} - F^2_{ij}}{N^2(N - 1)} \equiv s^2_{ij} \tag{29}$$

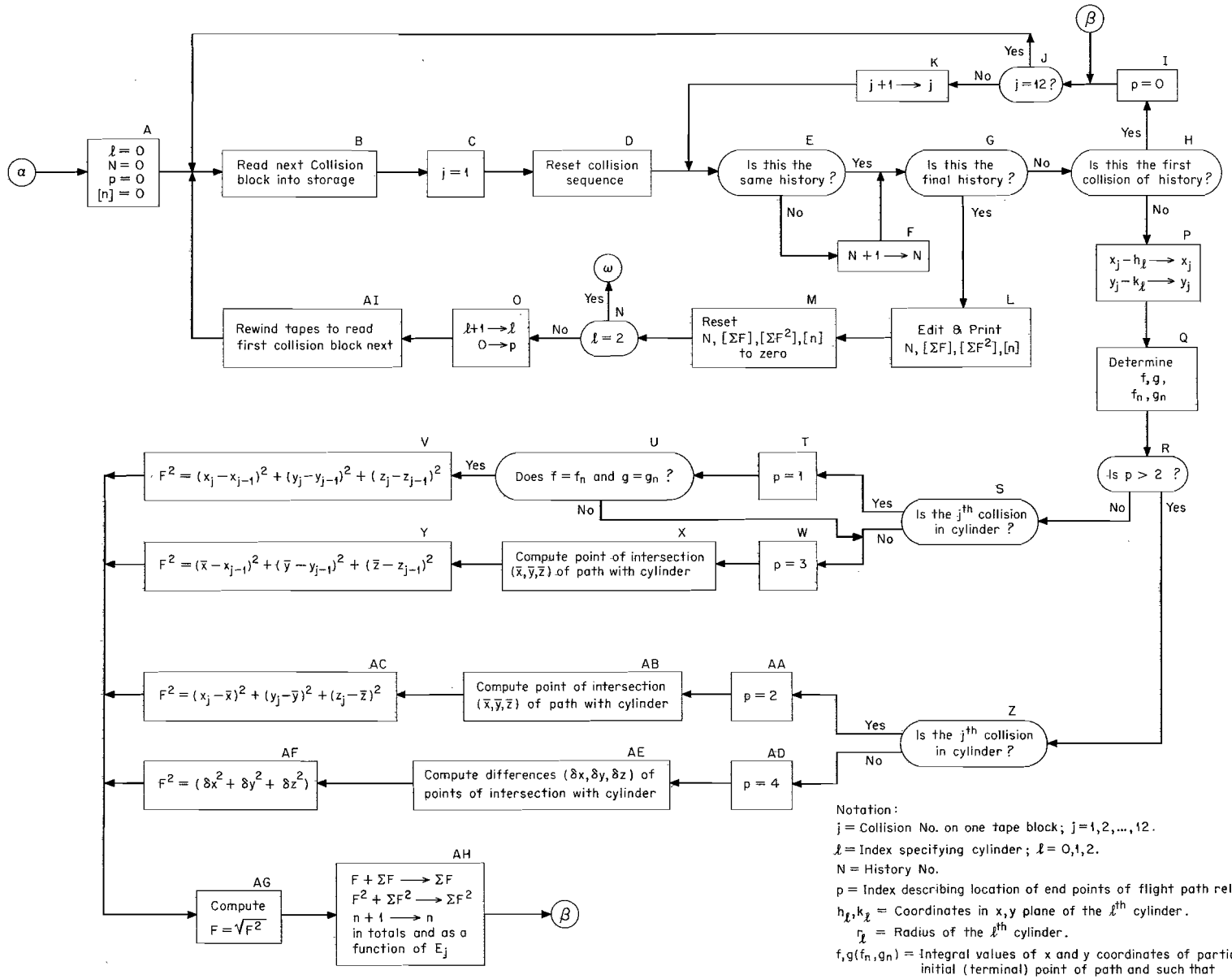

Notation:

j = Collision No. on one tape block; j = 1, 2, ..., 12.

ℓ = Index specifying cylinder; ℓ = 0, 1, 2.

N = History No.

p = Index describing location of end points of flight path relative to being in a cylinder.

h_ℓ, k_ℓ = Coordinates in x, y plane of the ℓth cylinder.

r_ℓ = Radius of the ℓth cylinder.

f, g (f_n, g_n) = Integral values of x and y coordinates of particular cylinder closest to initial (terminal) point of path and such that

$x_{j-1} - r_\ell \leq f \leq f_n \leq x_j + r_\ell$

if $x_j \geq x_{j-1}$

and $x_{j-1} + r_\ell \geq f \geq f_n \geq x_j - r_\ell$

if $x_j < x_{j-1}$, and similarly for

y_{j-1}, y_j, g, and g_n.

Fig. 7. Schematic Flow Chart of Flux Determinations.

and similarly

$$s^2_{F_i/N} = \frac{N \sum_j \sum_k F^2_{ijk} - F^2_i}{N^2(N-1)} = s^2_i \quad . \tag{30}$$

Now

$$\frac{F_i}{N} = \frac{1}{N} \sum_{h \neq j} F_{ih} + \frac{F_{ij}}{N} \tag{31}$$

where F_{ih} and F_{ij} are uncorrelated when $h \neq j$. An approximation to the variance of R_{ij} is given by

$$\begin{aligned} s^2_{R_{ij}} &= R^2_{ij} \left[\frac{s^2_{ij}}{F^2_{ij}/N^2} + \frac{s^2_i}{F^2_i/N^2} - \frac{2s^2_{ij}}{F_i \; F_{ij}/N^2} \right] \\ &= N^2 \, R^2_{ij} \left[\frac{s^2_{ij}}{F_{ij}} \left(\frac{1}{F_{ij}} - \frac{2}{F_i} \right) + \frac{s^2_i}{F^2_i} \right] . \end{aligned} \tag{32}$$

Finally, one may define ψ_{ij} as the proportionate flux per unit energy in energy interval $\triangle E_j$ in region i . Thus

$$\psi_{ij} = \frac{R_{ij}}{\triangle E_j} \tag{33}$$

and

$$s^2_{\psi_{ij}} = \left(\frac{1}{\Delta E_j}\right)^2 s^2_{R_{ij}} \quad . \tag{34}$$

The relative error or coefficient of variation of ψ_{ij} is

$$(CV)_{\psi_{ij}} = \frac{s_{\psi_{ij}}}{\psi_{ij}} \quad . \tag{35}$$

The results of the calculations are exhibited in Table II.

Table II

Estimated Proportion of Flux per Mev in Three Regions of the ORNL Graphite Reactor in Various Energy Intervals

Energy Interval	Region I		Region II		Region III	
	ψ_I	$(CV)_{\psi_I}$ (%)	ψ_{II}	$(CV)_{\psi_{II}}$ (%)	ψ_{III}	$(CV)_{\psi_{III}}$ (%)
.0250 - .05	8.232	2.31	6.648	2.22	8.510	2.60
.0500 - .1	3.260	1.34	2.575	2.56	3.061	2.18
.1000 - .25	1.461	1.75	1.235	2.24	1.515	1.91
.2500 - .5	.544	2.13	.566	2.32	.502	2.51
.5 - 1.0	.272	2.12	.316	2.62	.280	2.31
1.0 - 2.0	.092	2.80	.155	2.58	.092	3.13
2.0 - 3.0	.033	5.25	.043	5.38	.034	5.72
3.0 - 4.0	.0045	16.58	.013	12.82	.0042	19.38
4.0 - 5.0	.0062	12.45	.0050	15.72	.0069	13.25

Table II (Cont.)

Energy Interval	Region I		Region II		Region III	
	ψ_1	$(CV)_{\psi_I}$ (%)	ψ_{II}	$(CV)_{\psi_{II}}$ (%)	ψ_{III}	$(CV)_{\psi_{III}}$ (%)
5.0 - 6.0	-	-	-	-	-	-
6.0 - 7.0	.0029	18.45	.0039	18.68	.0035	18.43
7.0 - 8.0	-	-	-	-	-	-
8.0 - 9.0	.0010	31.42	-	-	.0013	31.42
9.0 -10.0	-	-	-	-	-	-

Let $\psi_i(E)\,dE$ be the proportion of the total flux per unit energy in region i due to neutrons with energy between E and $E + dE$. Then

$$R_{ij} = \int_{E \in \Delta E_j} \psi_i(E)\,dE \quad . \tag{36}$$

The proportion of the total fast flux, R_i^*, in region i due to neutrons with energy between E_1^* and E_2^* is then

$$R_i^* = \int_{E_1^*}^{E_2^*} \psi_i(E)\,dE \quad . \tag{37}$$

The analytical form of the function $\psi_i(E)$ is not given, but its graph may be approximated by the ψ_{ij}'s that were calculated.

If, instead of $\psi(E)$, one considers $\psi(u)$, where $u = \ln \frac{E_o}{E}$ is the lethargy and E_o is some constant, then one may tabulate the proportion of the

total fast flux per unit lethargy. The relationship between $\psi(E)$ and $\psi(u)$ is

$$\psi(u) = \psi(E) \left| \frac{\triangle E}{\triangle u} \right| = \psi(E) \left| \frac{E_2 - E_1}{\ln E_1 - \ln E_2} \right| . \tag{38}$$

Equation (37) may be replaced by

$$R_i^* = \int_{E_1^*}^{E_2^*} \psi_i(u)\, du \tag{39}$$

and evaluated graphically. Figure 8 contains the histogram formed by plotting the estimates obtained for $\psi_I(u)$ against the lethargy interval. E_o is taken to be 10 Mev. Table III contains the values of $\psi(u)$ for all three regions. It should be noted that lethargy is inversely related to the energy.

Acknowledgement

The assistance of E. B. Carter and H. B. Goertzel in the planning and execution of the IBM procedures, of Mrs. S. E. Atta in coding the UNIVAC procedure, and of Miss N. D. Given in compiling some of the summaries from the UNIVAC tapes is gratefully acknowledged.

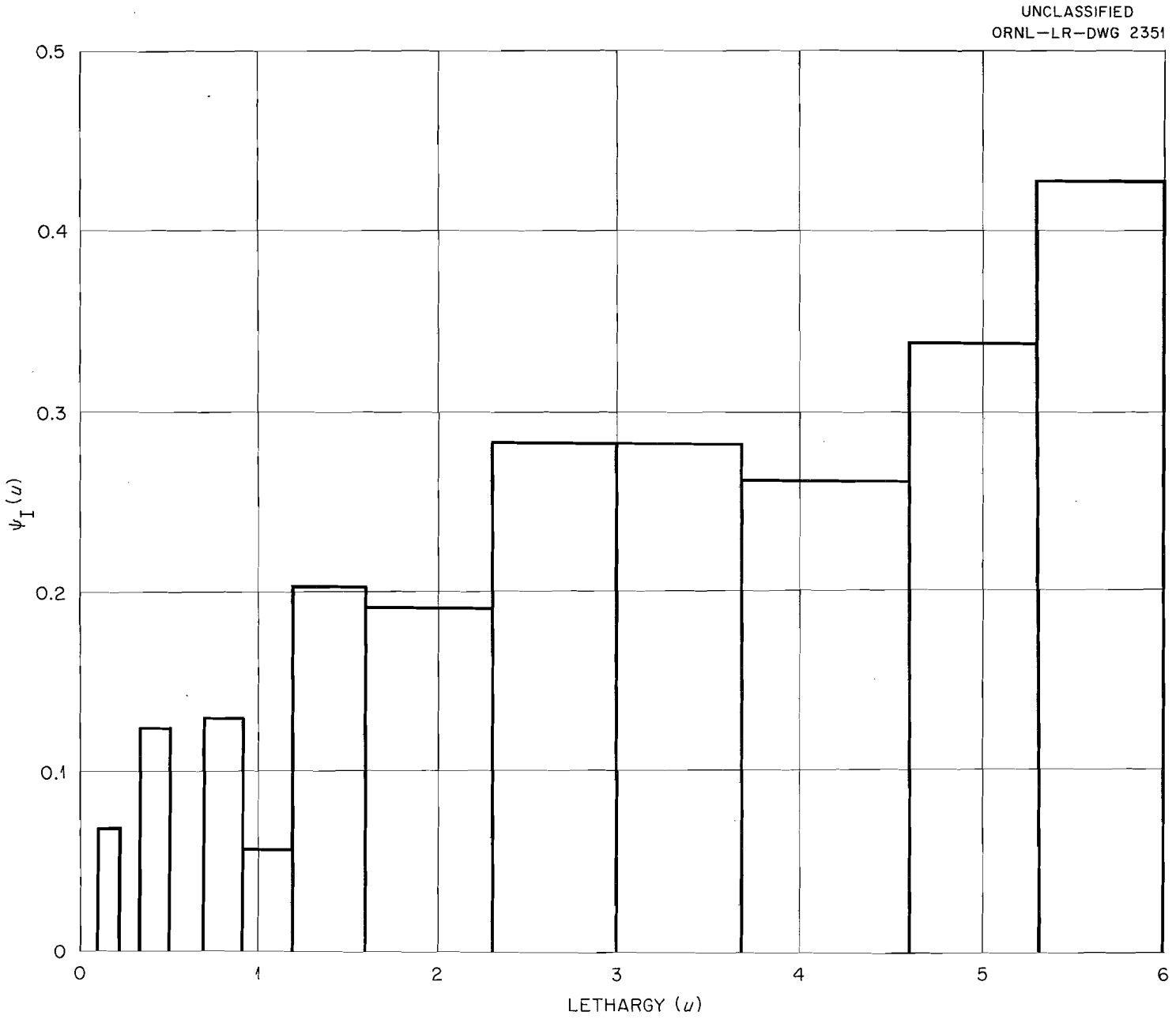

Fig. 8. Estimated Flux per Unit Lethargy in Region I.

[redacted]

Table III

Estimated Proportion of Flux per Unit Lethargy in Three Regions of the ORNL Graphite Reactor in Various Lethargy Intervals

Lethargy Interval	$\psi_I(u)$	$\psi_{II}(u)$	$\psi_{III}(u)$
0 - .104	-	-	-
.104 - .223	.008	-	.011
.223 - .357	-	-	-
.357 - .511	.019	.025	.023
.511 - .693	-	-	-
.693 - .916	.028	.022	.031
.916 - 1.204	.016	.046	.015
1.204 - 1.609	.082	.106	.084
1.609 - 2.303	.132	.223	.132
2.303 - 2.996	.196	.228	.202
2.996 - 3.689	.196	.204	.181
3.689 - 4.605	.240	.203	.248
4.605 - 5.298	.235	.185	.220
5.298 - 5.991	.296	.239	.306

REFERENCES

1. "Tables of Neutron Cross Sections for Elements P_o - C_m", compiled by G. Haines and K. Way, ORNL-86, 1948.

2. D. K. Holmes, Unpublished memorandum, June 15, 1950.

3. "Project Handbook", revised edition, CL-697, 1945.

4. J. Moshman, "The Generation of Pseudo-Random Numbers on a Decimal Calculator", Journal of the Association for Computing Machinery, Vol. 1 (1954), pp. 88-91.

JM:ih